A Phase-Shifting Based Human Gait Phase Estimation for Powered Transfemoral Prostheses

Woolim Hong, Namita Anil Kumar, and Pilwon Hur

***Abstract*—Phase variables are continuous real-valued functions which parameterize the gait cycle. As such, they can be used to estimate a powered prosthesis user's walking state. It is common to represent the phase variable as a function of the thigh angle. This approach assumes the thigh angle profile and its integral to be sinusoids. However, this assumption does not hold at lower walking speeds which leads to inaccurate heel-strike detection. In this study, we show that the thigh angle and its integral are phase-shifted from the ideal sinusoids by analyzing both able-bodied and amputee subject walking data. We then propose a novel phase variable incorporating phase-shift that is accurate even at lower walking speeds. We tested two variants of the proposed phase-shifted phase variable on a transfemoral prosthesis in an emulator study. Results show that phase-shifting improves heel-strike detection. Additionally, phase-shifting improves the linearity of the phase variable over the gait cycle. Analysis of the knee and ankle phase portraits showed that phase-shifting results in less deviations from the limit cycle.**

***Index Terms*—Wearable robotics, prosthetics and exoskeletons, gait phase estimation.**

I. Introduction

POWERED prostheses can improve the quality of life for lower-limb amputees by enhancing their physical [1]–[5] and psychological [6], [7] capabilities. Over the years, research into control frameworks for powered prosthesis mimicking healthy human gait kinematics and kinetics has soared [8]–[15]. A finite-state machine with impedance-based control is one approach to prosthesis control [8]–[11]. By modulating sets of impedance parameters (i.e., stiffness, damping and equilibrium angle) based on user's joint kinematics and kinetics, this control framework provides more control to the user and some force feedback. However, it requires a demanding tuning process due to a large set of impedance parameters [8]–[11]. To lessen tuning, many have used a tracking-based control framework [16]–[19]. This framework uses a parameterized variable over the gait cycle, but this approach may compromise user comfort by forcing the user to strictly follow pre-defined trajectories. To combine the merits of impedance control and tracking control, some researchers use a hybrid approach of an impedance control (stance phase) and a tracking control (swing phase) [20]–[22]. For instance, in [20], [21], stiffness and damping coefficients are given as a continuous function of the gait progression during the stance phase while the desired trajectories are generated based on the gait progression in the swing phase. Whether a tracking controller or a hybrid controller, estimating the user gait phase is crucial to synchronize the control of the prosthesis with the user.

A. Background

One approach to estimate the user gait phase is to use a kinematic variable (i.e., phase variable) that uniquely changes during locomotion [18]–[20], [23]–[25]. This variable can tell the user's walking progression regardless of time by parameterizing the entire gait cycle based on kinematic changes. Thus, the phase variable enables the prosthesis to track the user's walking state and provide the corresponding control signals. The phase variable has been derived using different kinematic information: tibia angle [23], linearized hip position [18], [19], and thigh angle [24], [25]. According to the related studies, to be used as the phase variable, it must be i) monotonic and bounded on [0,1] over time [24]–[28] and ii) purely controlled by the user [18], [19], [27]. The monotonicity and the boundedness guarantee a bijective mapping from the phase variable into 0-100% of the gait cycle (see Fig. 1). To have a full user authority implies a phase variable should be determined by the user's actions and not the prosthetic. The following are notable computations of phase variable using different types of kinematic data for a prosthesis control.

Tibia angle: Introduced by Holgate *et. al.* [23], the tibia angle profile can be divided into two parts at roughly 70% of the gait cycle. Each divided part satisfies the requirements for user autonomy, monotonicity and boundedness. This phase variable enables the user to control the prosthesis in a continuous manner. However, the tibia information can be used only with transtibial (below knee) amputees and not with transfemoral (above knee) amputees. Thus, this phase variable is limited to transtibial prostheses.

Linearized hip position: In transfemoral prosthesis control, a linearized hip position was used as the phase variable by the researchers [18], [19], [29]. This variable is a function of the user's horizontal hip position, calculated by inverse kinematics

Manuscript received October 15, 2020; accepted February 25, 2021. Date of publication March 25, 2021; date of current version April 22, 2021. This letter was recommended for publication by Associate Editor J.-J. Cabibihan and Editor P. Valdastri upon evaluation of the reviewers' comments. *(Corresponding author: Pilwon Hur.)*

Woolim Hong and Namita Anil Kumar are with the J. Mike Walker '66 Department of Mechanical Engineering, Texas A&M University, College Station, TX 77843 USA (e-mail: ulim8819@tamu.edu; namita.anilkumar@tamu.edu).

Pilwon Hur is with the School of Mechanical Engineering, Gwangju Institute of Science and Technology, Gwangju 61005, South Korea (e-mail: pilwonhur@gist.ac.kr).

This letter has supplementary downloadable material available at https://doi.org/10.1109/LRA.2021.3068907, provided by the authors.

Digital Object Identifier 10.1109/LRA.2021.3068907

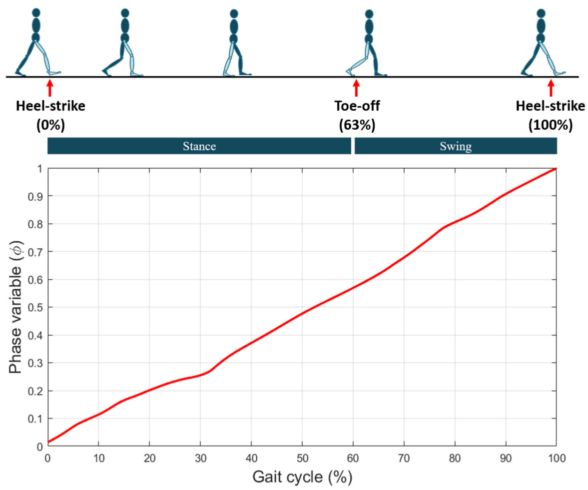

Fig. 1. A gait cycle is usually defined by a heel-strike to another heel-strike on the same leg. A phase variable (y-axis: $\Phi \in$ [0,1]) maps the gait cycle (x-axis: 0-100%) to [0,1].

using the user's shank and thigh information. During walking, the user's hip position shows a monotonic trend. However, to measure the shank and thigh angles, users must wear sensors (e.g., IMUs) on their intact side, which would discomfit the users. Additionally, by using the intact leg's data to control the prosthesis, the autonomy of the prosthetic limb is considerably limited.

Thigh angle: The thigh angle of the residual leg shows a periodic movement during the gait cycle [24]–[28]. Unlike the tibia angle, the residual thigh angle can be controlled by both transtibial and transfemoral amputees. This also eliminates the need for sensors on the intact limb. The resulting phase variable has shown reasonable estimation across different walking conditions: various speed [24], sloped terrains [20], [24], obstacle [5], and under perturbations [25]. Due to its simple implementation and consistency at different walking speeds, the thigh angle has been widely used in computing the phase variable for the transfemoral prosthesis control.

B. Contributions

While the thigh angle is a popular choice for phase variable computation, it is not perfect. Specifically, this approach assumes the thigh angle to be a cosine function, which is not true [25]–[27]. But, the effect of the dissimilarity (between the thigh angle and a cosine function) on phase variable computation has not been extensively investigated. We wish to fill this gap in knowledge in this letter. We hypothesize that phase-shifting the thigh angle profile overcomes the prior mentioned dissimilarity. Presented in Section III are four hypotheses that detail the benefits of phase-shifting. These hypotheses are proved through offline analysis of able-bodied and amputee subject walking data. We then propose and validate a novel phase-shifted phase variable and compare its performance to the conventional phase variable using thigh angle. This is done by real-time implementation on a powered transfemoral prosthesis (detailed in Section IV). The experimental results are reported in Section IV, and they are discussed in Section V. This study is concluded in Section VI.

II. Preliminaries

In this section, we briefly introduce the phase variable computing method using thigh information from previous studies [24]–[28]. These researchers made the following assumptions: i) A thigh profile $\theta(t)$ is a cosine-like function. ii) The integral of the thigh angle ($\Theta(t) = \int \theta(t)\, dt$) is a sine-like function. The phase portrait of thigh profile and its integral is an ellipse. Thus, a phase variable can be calculated using the arc-tangent function, as shown below.

$$\Phi(t) = \frac{1}{2\pi} atan2(k(\Theta(t) - \alpha), (\theta(t) - \beta)) \tag{1}$$

where the normalizing factors including the scale coefficient k, the amplitude shift of thigh integral α, and that of thigh angle β are defined by

$$k = \frac{|\theta_{max} - \theta_{min}|}{|\Theta_{max} - \Theta_{min}|},$$
$$\alpha = \frac{|\Theta_{max} + \Theta_{min}|}{2}, \quad \beta = \frac{|\theta_{max} + \theta_{min}|}{2}. \tag{2}$$

To make $\Phi(t)$ bounded on [0,1], the final $\Phi(t)$ is generated as below:

$$\Phi(t) = \begin{cases} \Phi(t) & \text{for } \Phi(t) \geq 0 \\ \Phi(t) + 1 & \text{for } \Phi(t) < 0 \end{cases} \tag{3}$$

The normalizing factors (k, α, and β) help center the phase portrait ($\theta(t)$ vs. $\Theta(t)$) around the origin, reducing the non-linearity of the phase variable. The integral value is initialized when the heel-strike occurs, and the normalizing factors are updated every quarter gait cycle to maintain the orbital radius in the gait cycle [24], [25]. For use throughout this letter, we name the phase variable resulting from this procedure as PV and symbolize it as $\Phi(t)$.

III. Methods

We propose a phase-shifted phase variable (PS-PV), computed using the prior mentioned PV and a new phase-shifting method. First, we state some hypotheses that form the foundation for the proposed method. These hypotheses are proved via an offline analysis of both able-bodied and amputee subject walking data. Finally, a real-time implementation of PS-PV for the powered prosthesis is explained.

Hypothesis 1: A thigh angle profile is a phase-shifted cosine-like function (see Fig. 2.A).

Hypothesis 2: A thigh integral is a phase-shifted sine-like function (see Fig. 2.B).

Hypothesis 3: By implementing a phase-shifting, the linearity of the phase variable will be increased. Note that a strictly linear phase variable is resulted when the ideal sinusoidal functions are given in phase variable calculation.

Hypothesis 4: After a phase-shifting implementation, the heel-strike detection error will be reduced.

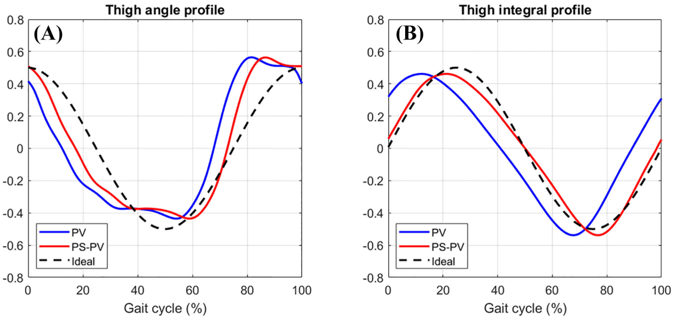

Fig. 2. An example of thigh angle and its integral profile over the gait cycle from a healthy subject. Black dashed lines indicate the ideal sinusoidal functions, while blue and red lines indicate the conventional thigh information and the phase-shifted thigh information, respectively. **(A)** Two thigh angle profiles (PV vs. PS-PV) and a cosine function, **(B)** Two thigh integral profiles (PV vs. PS-PV) and a sine function

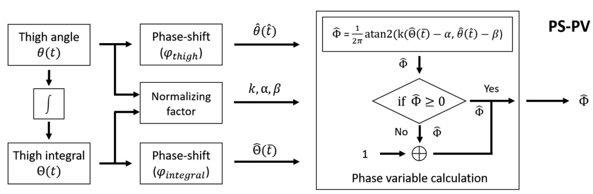

Fig. 3. Overview of phase-shifted phase variable (PS-PV) computation using thigh information. Phase-shifts for thigh (φ_{thigh}) and its integral ($\varphi_{integral}$) are respectively implemented.

A. Phase-Shifting Method

To validate the given hypotheses, we checked whether the thigh profile and its integral are phase-shifted from ideal sinusoids. To find the desired phase-shift for the best fitting to the ideal sinusoids, we utilized a cross-correlation technique, which is widely used in the field of signal processing for time delay detection. The obtained phase-shifts (thigh: φ_{thigh} and thigh integral: $\varphi_{integral}$) were used to obtain the phase-shifted thigh angle $\hat{\theta}(\hat{t})$ and the phase-shifted thigh integral $\hat{\Theta}(\bar{t})$ in Eq. 4 and Eq. 5 (see Fig. 3).

$$\hat{\theta}(\hat{t}) = \theta(t + \varphi_{thigh}) \tag{4}$$

$$\hat{\Theta}(\bar{t}) = \Theta(t + \varphi_{integral}) \tag{5}$$

The phase-shifted phase variable (PS-PV: $\hat{\Phi}(t)$) is calculated as follows.

The normalization factors (k, α, β) are the same as PV (given in Eq. 2).

$$\hat{\Phi}(t) = \frac{1}{2\pi} atan2(k(\hat{\Theta}(\bar{t}) - \alpha), (\hat{\theta}(\hat{t}) - \beta)). \tag{6}$$

B. Method Validation

We perform offline analysis using both able-bodied and amputee subject walking data for comparing our method with the conventional method. The evaluation process for each method is based on four metrics: i) cross-correlation between thigh angle and cosine function, ii) cross-correlation between thigh integral and sine function, iii) linearity of the phase variable, and iv) heel-strike detection error. The cross-correlation result indicates how similar the two functions are. The result is 1.0 if and only if the thigh angle profile (or its integral) is identical to the ideal cosine (or sine) function. We evaluate the linearity of the resulting phase variable of each method by comparing root-mean-square (RMS) error between the phase variable and a linear function over the gait cycle, which is bounded on [0, 1]. Heel-strike detection error is calculated in the percentage. Assuming the ideal heel-strike occurs at 100% of the gait cycle when the phase variable reaches its peak (i.e., 1.0), the heel-strike detection error indicates the deviation from this ideal maximum value of the phase variable.

TABLE I
THE MEAN AND A STANDARD DEVIATION OF THE FOUR METRICS ACROSS 50 CONSECUTIVE STEPS FOR THREE SUBJECTS

	Speed (m/s)	PV	PS-PV
Thigh angle correlation	0.5	0.862 ± 0.033	0.913 ± 0.014
	1.0	0.859 ± 0.037	0.935 ± 0.011
	1.5	0.783 ± 0.035	0.950 ± 0.008
	2.0	0.700 ± 0.036	0.949 ± 0.008
Thigh integral correlation	0.5	0.894 ± 0.036	0.988 ± 0.003
	1.0	0.876 ± 0.038	0.994 ± 0.002
	1.5	0.801 ± 0.035	0.993 ± 0.002
	2.0	0.720 ± 0.037	0.990 ± 0.002
Linearity error	0.5	0.040 ± 0.009	0.035 ± 0.007
	1.0	0.029 ± 0.006	0.024 ± 0.005
	1.5	0.025 ± 0.005	0.028 ± 0.007
	2.0	0.044 ± 0.007	0.046 ± 0.005
Heel-strike detection error	0.5	0.793 ± 0.760	0.736 ± 0.350
	1.0	0.706 ± 0.719	0.540 ± 0.272
	1.5	1.073 ± 0.949	0.667 ± 0.264
	2.0	2.063 ± 2.188	1.642 ± 0.411

1) Healthy subject walking: We collected walking data from three healthy subjects (males, 28.3 ± 1.5 yrs, 1.70 ± 0.15 m, 65.0 ± 3.0 kg). The experiment protocol was approved by the Institutional Review Board (IRB) at Texas A&M University (IRB2015-0607F). The subjects were asked to walk on a treadmill at four different speeds: 0.5, 1.0, 1.5, and 2.0 m/s. An Inertia Measurement Unit (IMU) mounted on the thigh measured their thigh angles. A force sensor mounted at the subjects' heel was used to detect the actual heel-strike. These heel-strikes were used to segment the walking data set. Over 50 steps were included in each trial.

Fig. 2 presents the thigh angle and thigh integral data of one subject. The phase-lag is evident in both thigh angle and its integral compared to the ideal cosine and sine functions, respectively. Therefore, having a leading phase for both thigh angle and thigh integral should improve correlation with the ideal sinusoidal functions. This idea is validated in the processed results reported in Table. I. We found the significant effect of walking speed on the method (PV or PS-PV) and the significant difference between the methods using two-way repeated ANOVA in RStudio statistical software (RStudio, Boston, MA, USA). With both PV and PS-PV, there is a significant effect of walking speed on the correlation metrics (i.e. correlation of thigh angle and thigh integral with ideal sinusoids), linearity error, and heel-strike detection error ($p < 0.05$). Specifically, correlation metrics reduced with walking speed, while the errors increased. Across all walking speeds, the correlation metrics increased from PV to PS-PV significantly ($p < 0.05$). Furthermore, this effect is even higher when the walking speed is increased. Heel-strike detection error consistently decreased

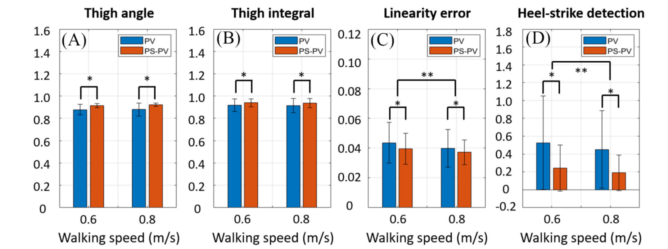

Fig. 4. Bar indicates mean value of each metric while error bar is given with ± 1 SD (blue: PV, red: PS-PV) **(A)** Cross-correlation between thigh profile and ideal cosine function, **(B)** Cross-correlation between thigh integral and ideal sine function, **(C)** Root-mean-square (RMS) error between the phase variable and a linear function, **(D)** Heel-strike detection error between the maximum phase variable value and the actual heel-strike (100%) * indicates a significant difference between PV and PS-PV. ** indicates a significant difference between two walking speeds.

with the implementation of phase-shifting, but this reduction was not significant. On the other hand, linearity errors improved with the application of phase-shifting only at lower walking speeds.

2) Amputee subject walking: Amputee walking kinematics is far different from that of a healthy human. Thus, the analysis of amputee walking data can provide solid support to the proposed idea. We used a publicly accessible biomechanics dataset from the University of Utah [30] to conduct a biomechanical analysis for amputee walking. This dataset contains 18 unilateral transfemoral amputees' walking at five different walking speeds. On the basis of their comfortable walking (0.8 m/s), the amputee subjects were divided into two groups: K2 (limited community ambulators) and K3 (full community ambulators) [30]. Each group has nine members and walked at different walking speeds, K2: 0.4, 0.5, 0.6, 0.7, 0.8 m/s and K3: 0.6, 0.8, 1.0, 1.2, 1.4 m/s. Using the given dataset, the four metrics were assessed.

Three-way mixed ANOVA was performed for each result in RStudio to find significant differences between given factors (group, walking speed, and method). To encompass two groups, we chose the overlapped walking speed (0.6 and 0.8 m/s) for the statistical analysis. One of the subjects in K2 group has no walking data at 0.8 m/s [30], this subject was thus excluded. According to the result, no interaction effect was found between each given factor ($p > 0.05$). There was no significant difference between two groups for all metrics ($p > 0.05$). We found significant differences between methods (PV vs. PS-PV) for all four metrics in Fig. 4 (A^*: $p = 0.004$, B^*: $p = 0.001$, C^*: $p = 0.02$, D^*: $p = 2.58\text{e-}05$). For both linearity error and heel-strike detection error, significant differences were found between walking speeds: 0.6 and 0.8 m/s (Fig. 4. C^{**}: $p = 0.002$, D^{**}: $p = 0.002$). In other words, phase-shifting significantly improved all four metrics. i) The thigh angle correlation increased by 4.2% and 4.8% at two different walking speeds, respectively (Fig. 4.A). ii) Thigh integral correlation also increased by 2.4% and 2.5% at each walking speed in Fig. 4.B. iii) Fig. 4.C shows that the linearity errors are decreased by 9.5% and 6.9%. iv) Heel-strike detection error drastically decreased by 53.8% and 58.0% for each walking speed (see Fig. 4.D).

Thus, Hypothesis 1 and 2 (Section III) are validated across all different walking speeds in both the able-bodied and amputee subject. Hypothesis 4 is also validated in both healthy and

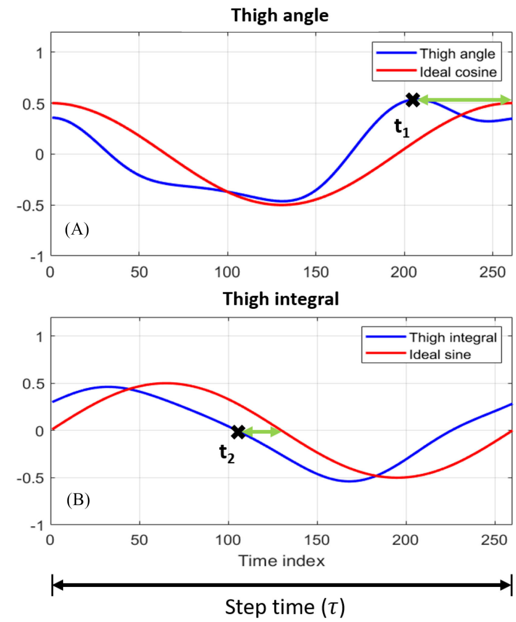

Fig. 5. **(A)** Phase-shift in thigh angle: $\varphi_1 = \tau - t_1$, and **(B)** Phase-shift in thigh integral: $\varphi_2 = \tau/2 - t_2$. Blue lines indicate thigh information, while red lines indicate ideal sinusoids.

amputee walking results. In the case of Hypothesis 3, we found the linearity error decreased after implementing phase-shifting in amputee subject. In the case of healthy subject, however, the linearity error decreased at 0.5 and 1.0 m/s, but increased at 1.5 and 2.0 m/s when phase-shifting was implemented.

C. Real-Time Phase-Shifting Implementation

1) Phase-shift detection: In Section III.A, we found the optimal phase-shift by using a cross-correlation for the best fitting sinusoidal functions. Yet, this cannot be achieved during real-time prosthetic control. We thus need to detect the phase delay during the prosthetic's operation. We propose two references for phase delay, illustrated in Fig. 5.

Reference 1: We find the phase-shift (φ_1) between the peaks in the thigh angle profile (labeled t_1 in Fig. 5.A) and the ideal cosine function (corresponds to heel-strike).

Reference 2: We find the lag (φ_2) between zero-crossing point from positive to negative (t_2) in the thigh integral and the half-way mark (or half the step time) (Fig. 5.B.)

$$\varphi_1 = \tau - t_1, \quad \varphi_2 = \frac{1}{2}\tau - t_2 \tag{7}$$

2) Phase variable calculation: We update Eq. 4 using φ_1 as shown in Eq. 8. Note that the phase-shifted thigh integral can be computed in two ways: i) by using the phase-shift φ_2 to get $\hat{\Theta}_1(\bar{t})$ (refer Eq. 9), ii) by evaluating the integral of $\hat{\theta}(\hat{t})$ (refer Eq. 10). These two methods would differ because the thigh angle $\theta(t)$ is not an ideal cosine function.

$$\hat{\theta}(\hat{t}) = \theta(t + \varphi_1) \tag{8}$$

$$\hat{\Theta}_1(\bar{t}) = \Theta(t + \varphi_2) \tag{9}$$

$$\hat{\Theta}_2(\hat{t}) = \int \hat{\theta}(\hat{t})\, d\hat{t} \tag{10}$$

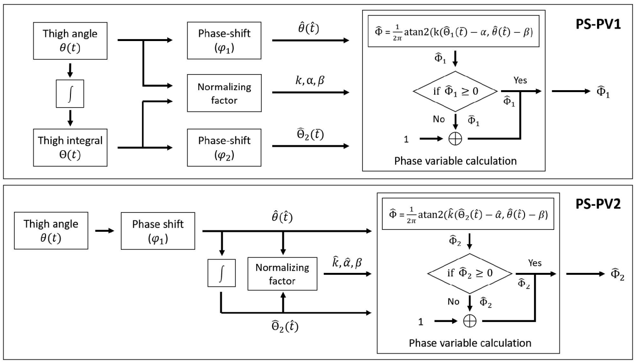

Fig. 6. Overview of phase variable computation using the proposed method. Resulting phase variables are PS-PV1: $\hat{\Phi}_1(t)$ and PS-PV2: $\hat{\Phi}_2(t)$

We investigate both methods in the following sections (shown in Fig. 6). The phase variable using Eq. 9 is called PS-PV1 and symbolized by $\hat{\Phi}_1(t)$, while the one using Eq. 10 is called PS-PV2 and uses the symbol $\hat{\Phi}_2(t)$.

$$\hat{\Phi}_1(t) = \frac{1}{2\pi} atan2(k(\hat{\Theta}_1(\bar{t}) - \alpha), (\hat{\theta}(\hat{t}) - \beta)) \tag{11}$$

$$\hat{\Phi}_2(t) = \frac{1}{2\pi} atan2(\hat{k}(\hat{\Theta}_2(\hat{t}) - \hat{\alpha}), (\hat{\theta}(\hat{t}) - \beta)) \tag{12}$$

In the case of PS-PV2, we must use different normalization factors for the thigh integral $\hat{\Theta}_2(\hat{t})$:

$$\hat{k} = \frac{|\hat{\theta}_{max} - \hat{\theta}_{min}|}{|\hat{\Theta}_{2,max} - \hat{\Theta}_{2,min}|}, \quad \hat{\alpha} = \frac{|\hat{\Theta}_{2,max} + \hat{\Theta}_{2,min}|}{2} \tag{13}$$

All normalizing factors are updated via a weighted sum of their prior values (computed during previous gait cycles). Accounting for the history of these factors provides for more stable walking. The weighting is a forgetting factor $e^{-\Delta t}$, where Δt is the time elapsed since the time of recording the corresponding value.

IV. Results

A. Experimental Setup and Protocol

To validate the proposed idea in real-time, a treadmill walking experiment was designed using a fully actuated transfemoral prosthesis–AMPRO II, depicted in Fig. 7. To provide human-like ambulation to the user, the ankle joint was controlled by an impedance controller [21] while the knee joint was controlled by a hybrid of impedance (stance phase) and tracking controller (swing phase) [20]. An IMU mounted on the thigh of the prosthesis side (Fig. 7.A) was used to detect the user's thigh motion. The prosthesis was operated under a state-based control scheme using the three different phase variables presented in this letter: PV, PS-PV1, and PS-PV2. A force sensor under the heel (Fig. 7.F) was used to initialize the gait cycle and the control parameters. The actual joint angles were collected by two high-resolution optical encoders at each joint.

A healthy young subject (male, 1.70 m, 70 kg) participated in the experiment using a L-shape adapter for emulating a prosthetic walking. The subject was asked to walk on the treadmill at his comfortable walking speed (0.80 m/s). During the

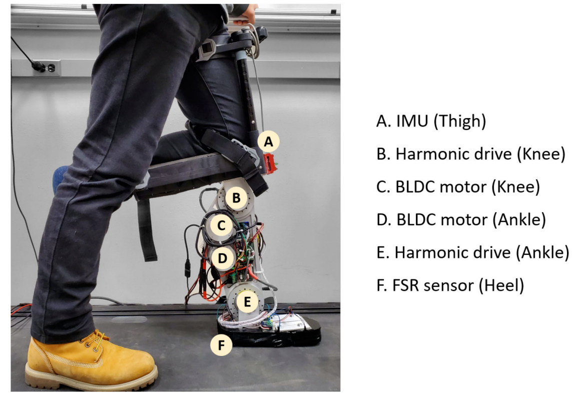

Fig. 7. AMPRO II–a custom-built powered transfemoral prosthesis at Texas A&M University

TABLE II
CORRELATION RESULTS OF PROSTHETIC WALKING USING THREE DIFFERENT METHODS: THIGH ANGLE AND ITS INTEGRAL

	PV	PS-PV1	PS-PV2
Thigh angle	0.86 ± 0.03	0.89 ± 0.02	
Thigh integral	0.90 ± 0.05	0.90 ± 0.06	0.91 ± 0.05

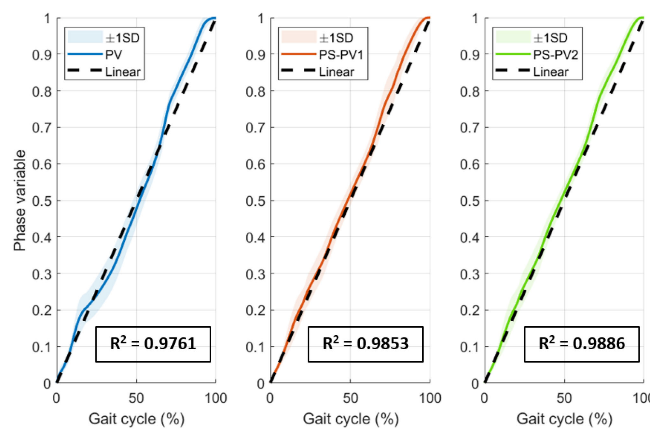

Fig. 8. Resulting phase variable using three different methods (blue: PV, red: PS-PV1, green: PS-PV2). While the solid lines represent the mean of 15 consecutive steps, the shaded regions indicate ±1 standard deviation. Black dashed lines indicate the linear function over the gait cycle.

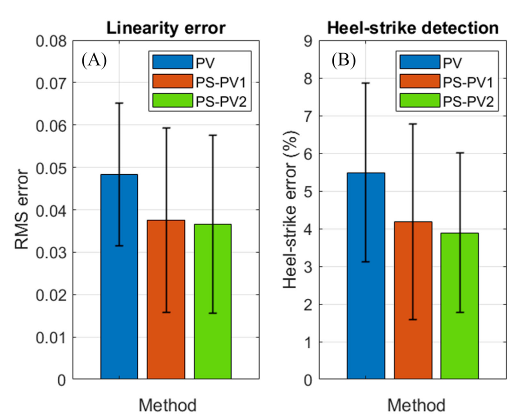

Fig. 9. **(A)** RMS error between the phase variable and a linear function. **(B)** Heel-strike detection error (%). (blue: PV, red: PS-PV1, green: PS-PV2). Error bars indicate ±1 s.d.

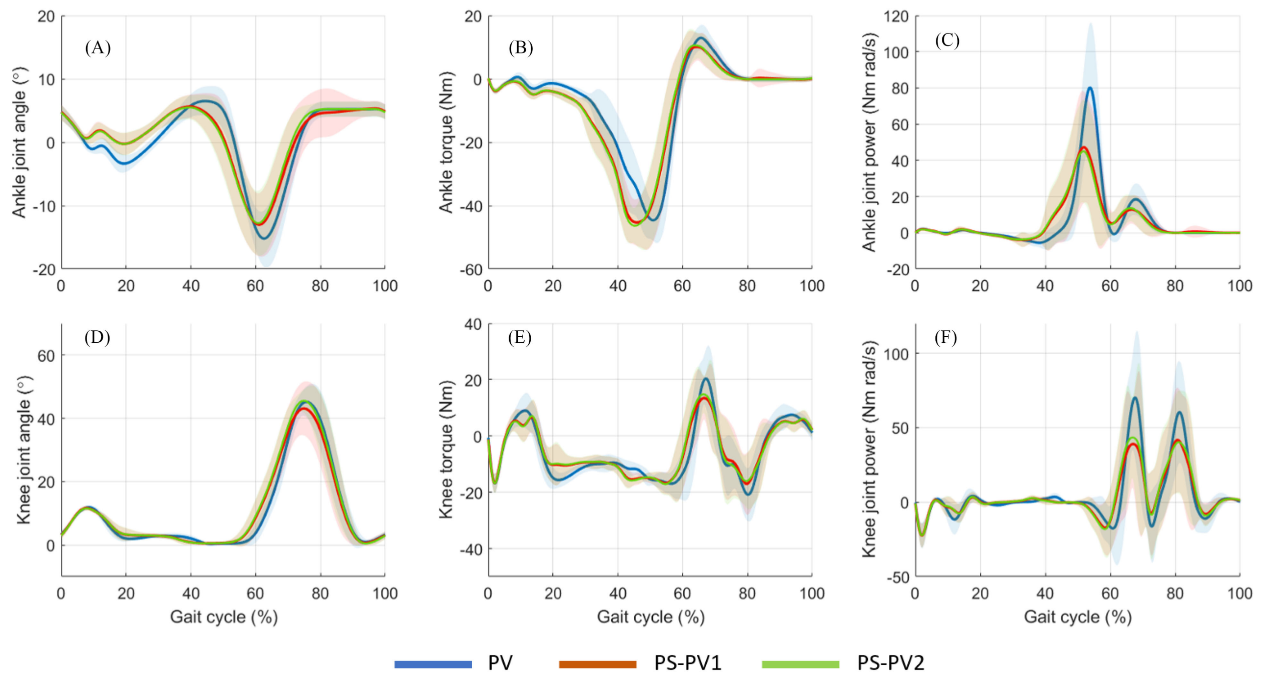

Fig. 10. Joint kinematics/kinetics results (top: ankle, bottom: knee) using the three phase variables: blue: PV, red: PS-PV1, green: PS-PV2. The solid lines and the shaded regions indicate the mean and ±1 standard deviation of 15 consecutive steps, respectively.

experiment, safety was assured by handrails on either side of the treadmill. The experiment protocol was approved by the Institutional Review Board (IRB) at Texas A&M University (IRB2015-0607F).

B. Method Comparison

As shown in Table. II, the correlation results of both thigh angle and its integral increased when the phase-shifting methods (PS-PV1 and PS-PV2) were implemented for prosthetic control. The resulting phase variables (i.e., PV, PS-PV1, and PS-PV2) are reported in Fig. 8. First, all three of phase variables show a reliable estimation result over the entire gait cycle, obeying the aforementioned properties (Section I.A). Compared to the previous method (PV: $R^2 = 0.9761$), a higher linearity is observed in both results of phase-shifting method (PS-PV1: $R^2 = 0.9853$, PS-PV2: $R^2 = 0.9886$). This fact is further strengthened by Fig. 9. A which shows a decrease in RMS error between the resulting phase variable and a linear function when the phase-shifting is implemented. The error of heel-strike detection in PV is 5.5%, while those of PS-PV1 and PS-PV2 are 4.2% and 3.9%, respectively (see Fig. 9.B).

C. Joint Kinematics/Kinetics Comparison

Fig. 10 presents the prosthetic joint kinematics/kinetics results. Compared to both phase-shifting methods, larger ankle dorsiflexion and knee-flexion was observed in PV (see Fig. 10.A and D). Fig. 10.C and F also show extensive push-off power in PV. Interestingly, these results can be attributed to the aforementioned linearity of the phase variable. According to the result in Fig. 8, from 65% to 70% of the gait cycle, PV has a steeper slope than others. Since this region is in the middle of the swing phase, this steeper slope leads to accelerated joint movements and an unwillingly high push-off. This is clearly shown in the supplemental video [31]. PS-PV2 has a slightly steeper slope than PS-PV1 (Fig. 8). Accordingly, we notice slightly high knee-flexion in PS-PV2 compared to PS-PV1.

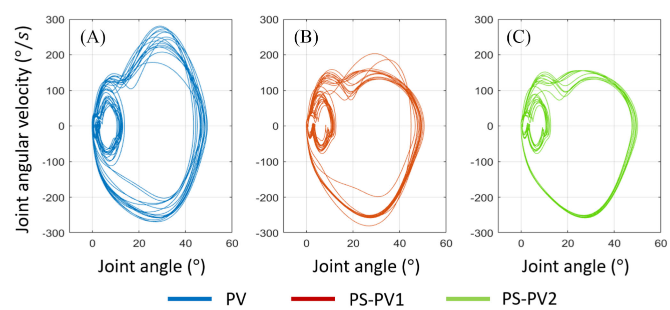

Fig. 11. Phase portrait (joint angle vs. joint velocity) of the knee for 15 consecutive steps (blue: PV, red: PS-PV1, green: PS-PV2)

V. Discussion

To analyze the stability of each method, the phase portraits of the knee joint were analyzed (Fig. 11). A clear limit cycle can be identified in each phase portrait. Interestingly, lesser deviations from the limit cycle were observed in PS-PV1 and PS-PV2. Qualitatively, we can see that PS-PV2 had the least deviation from the limit cycle, followed by PS-PV1, while PV had the most. We also tried to quantify this result using Lyapunov exponent (LE). LE measures the sensitivity to initial conditions by quantifying the exponential rates of convergence (or divergence) of the trajectory [32], [33]. For instance, the deviation from the limit cycle converges to zero when LE is negative. The magnitude of LE refers to the rate of convergence. Thus, the largest LE (the dominant value) is often utilized as a measure of the local instability of the system [34]–[36]. We used Kantz algorithm [36], [37] to calculate the maximum LE based on the Euclidean distance from the limit cycle. We consider averaged phase portrait of 15 steps as the limit cycle. The LE was the smallest for PS-PV2 (ankle: -0.0340, knee: -0.0805), followed by PS-PV1 (ankle: 0.0185, knee: -0.0205), and finally PV (ankle: 0.0244, knee: 0.0123). Due to the limited number of subjects, it is hard to draw any statistical conclusion. However, we could highlight some obvious trends. PS-PV1 and PS-PV2 showed smaller LE values than PV, implying that PS-PV1 and PS-PV2 provide more stable and robust control compared to PV. Finally, note that PS-PV2 has the lowest linearity error, heel-strike detection error, and deviations from its limit cycle. We caveat this result with the limited sample size for this study.

Due to the limited torque of the motors, we limited the walking speed to 0.80 m/s, which is slower than normal human walking. More walking experiments will be conducted at different walking speeds in the future. Owing to the use of an L-shape simulator and a height difference between the two limbs, slightly higher hip extensions were observed from the prosthesis side during the experiment. This could affect the thigh kinematics and the resulting phase variable. However, the affected thigh angle still has a phase-shift from the ideal cosine function, so the proposed method still holds.

The amount of phase-shift could vary according to users since individuals show different joint kinematics during walking. [30], [38]. Thus, it is reasonable to claim that the required phase-shift is user specific. We could thus develop a learning based gait phase estimation model using the proposed phase-shifted phase variable. Due to the world-wide COVID-19 pandemic, there were challenges in conducting the amputee walking experiments. We hope to accomplish this in the future with a larger sample size of amputee subjects. The test will also be conducted at varying walking speeds to see how the proposed method affects the amputees' metabolic cost.

VI. Conclusion

In this study, we propose a phase-shifted phase variable using the user's thigh information. It is shown that the thigh angle profile and its integral are phase-shifted sinusoids. Applying phase-shifts to the thigh angle and integral profiles improve linearity and heel-strike detection in the resulting phase variable. A real-time implementation of this phase variable was proposed and tested on a transfemoral prosthesis in an emulator study. Similar to the offline analysis, application of phase-shifting made the resulting phase variable more linear. A key benefit of a linear phase variable is more controlled push-off assistance (highlighted in the supplemental video [31]). Analysis of the phase portrait of the knee and ankle revealed that the phase-shifted phase variables had fewer deviations from the limit cycle when the proposed method was applied. For real-time implementation, preliminary results suggest computing the phase variable using the integral of the phase-shifted thigh angle rather than having a dedicated thigh integral phase-shift. We conclude that the proposed phase-shifted phase variable enables more accurate gait progress detection and thus more robust walking.

Acknowledgment

The authors would like to thank Kenny Chour for his assistance.

References

[1] S. K. Au, H. Herr, J. Weber, and E. C. Martinez-Villalpando, "Powered ankle-foot prosthesis for the improvement of amputee ambulation," in *Proc. 29th Annu. Int. Conf. IEEE Eng. Med. Biol. Soc.*, Aug. 2007, pp. 3020–3026.

[2] F. Sup, H. A. Varol, and M. Goldfarb, "Upslope walking with a powered knee and ankle prosthesis: Initial results with an amputee subject," *IEEE Trans. Neural Syst. Rehabil. Eng.*, vol. 19, no. 1, pp. 71–78, Feb. 2011.

[3] N. Thatte and H. Geyer, "Towards local reflexive control of a powered transfemoral prosthesis for robust amputee push and trip recovery," in *Proc. IEEE/RSJ Int. Conf. Intell. Robots Syst.*, Sep. 2014, pp. 2069–2074.

[4] E. D. Ledoux and M. Goldfarb, "Control and evaluation of a powered transfemoral prosthesis for stair ascent," *IEEE Trans. Neural Syst. Rehabil. Eng.*, vol. 25, no. 7, pp. 917–924, Jul. 2017.

[5] J. Mendez, S. Hood, A. Gunnel, and T. Lenzi, "Powered knee and ankle prosthesis with indirect volitional swing control enables level-ground walking and crossing over obstacles," *Sci. Robot.*, vol. 5, no. 44, 2020.

[6] T. Pohjolainen, H. Alaranta, and M. Kärkäinen, "Prosthetic use and functional and social outcome following major lower limb amputation," *Prosthetics Orthotics Int.*, vol. 14, no. 2, pp. 75–79, 1990.

[7] W. C. Miller, A. B. Deathe, M. Speechley, and J. Koval, "The influence of falling, fear of falling, and balance confidence on prosthetic mobility and social activity among individuals with a lower extremity amputation," *Arch. Phys. Med. Rehabil.*, vol. 82, no. 9, pp. 1238–1244, 2001.

[8] F. Sup, A. Bohara, and M. Goldfarb, "Design and control of a powered transfemoral prosthesis," *Int. J. Robot. Res.*, vol. 27, no. 2, pp. 263–273, 2008.

[9] D. Wang, M. Liu, F. Zhang, and H. Huang, "Design of an expert system to automatically calibrate impedance control for powered knee prostheses," in *Proc. IEEE 13th Int. Conf. Rehabil. Robot.*, 2013, pp. 1–5.

[10] A. M. Simon *et al.*, "Configuring a powered knee and ankle prosthesis for transfemoral amputees within five specific ambulation modes," *PLoS One*, vol. 9, no. 6, 2014, Paper. e 99387.

[11] N. P. Fey, A. M. Simon, A. J. Young, and L. J. Hargrove, "Controlling knee swing initiation and ankle plantarflexion with an active prosthesis on level and inclined surfaces at variable walking speeds," *IEEE J. Transl. Eng. Health Med.*, vol. 2, pp. 1–12, 2014.

[12] V. Azimi, T. Shu, H. Zhao, E. Ambrose, A. D. Ames, and D. Simon, "Robust control of a powered transfemoral prosthesis device with experimental verification," in *Proc. Amer. Control Conf.*, May 2017, pp. 517–522.

[13] T. Lenzi, M. Cempini, J. Newkirk, L. J. Hargrove, and T. A. Kuiken, "A lightweight robotic ankle prosthesis with non-backdrivable cam-based transmission," in *Proc. IEEE 15th Int. Conf. Rehabil. Robot.*, Jul. 2017, pp. 1142–1147.

[14] T. Elery, S. Rezazadeh, C. Nesler, J. Doan, H. Zhu, and R. D. Gregg, "Design and benchtop validation of a powered knee-ankle prosthesis with high-torque, low-impedance actuators," in *Proc. IEEE Int. Conf. Robot. Automat.*, May 2018, pp. 2788–2795.

[15] A. F. Azocar, L. M. Mooney, L. J. Hargrove, and E. J. Rouse, "Design and characterization of an open-source robotic leg prosthesis," in *Proc. 7th IEEE Int. Conf. Biomed. Robot. Biomechatron.*, Aug. 2018, pp. 111–118.

[16] R. D. Gregg, T. Lenzi, L. J. Hargrove, and J. W. Sensinger, "Virtual constraint control of a powered prosthetic leg: From simulation to experiments with transfemoral amputees," *IEEE Trans. Robot.*, vol. 30, no. 6, pp. 1455–1471, Dec. 2014.

[17] A. E. Martin and R. D. Gregg, "Stable, robust hybrid zero dynamics control of powered lower-limb prostheses," *IEEE Trans. Autom. Control*, vol. 62, no. 8, pp. 3930–3942, Aug. 2017.

[18] V. Paredes, W. Hong, S. Patrick, and P. Hur, "Upslope walking with transfemoral prosthesis using optimization based spline generation," in *Proc. IEEE/RSJ Int. Conf. Intell. Robots Syst.*, Oct. 2016, pp. 3204–3211.

[19] H. Zhao, J. Horn, J. Reher, V. Paredes, and A. D. Ames, "First steps toward translating robotic walking to prostheses: A nonlinear optimization based control approach," *Auton. Robots*, vol. 41, no. 3, pp. 725–742, 2017.

[20] W. Hong, V. Paredes, K. Chao, S. Patrick, and P. Hur, "Consolidated control framework to control a powered transfemoral prosthesis over inclined terrain conditions," in *Proc. IEEE Int. Conf. Robot. Automat.*, May 2019, pp. 2838–2844.

[21] N. Anil Kumar, W. Hong, and P. Hur, "Impedance control of a transfemoral prosthesis using continuously varying ankle impedances and multiple equilibria," in *IEEE Int. Conf. Robot. Automat.*, 2020, pp. 1755–1761.

[22] B. E. Lawson, J. Mitchell, D. Truex, A. Shultz, E. Ledoux, and M. Goldfarb, "A robotic leg prosthesis: Design, control, and implementation," *IEEE Robot. Automat. Mag.*, vol. 21, no. 4, pp. 70–81, Dec. 2014.

[23] M. A. Holgate, T. G. Sugar, and A. W. Bohler, "A novel control algorithm for wearable robotics using phase plane invariants," in *Proc. IEEE Int. Conf. Robot. Automat.*, 2009, pp. 3845–3850.

[24] D. Quintero, D. J. Villarreal, D. J. Lambert, S. Kapp, and R. D. Gregg, "Continuous-phase control of a powered knee-ankle prosthesis: Amputee experiments across speeds and inclines," *IEEE Trans. Robot.*, vol. 34, no. 3, pp. 686–701, Jun. 2018.

[25] D. J. Villarreal, H. A. Poonawala, and R. D. Gregg, "A robust parameterization of human gait patterns across phase-shifting perturbations," *IEEE Trans. Neural Syst. Rehabil. Eng.*, vol. 25, no. 3, pp. 265–278, Mar. 2017.

[26] D. J. Villarreal and R. D. Gregg, "A survey of phase variable candidates of human locomotion," in *Proc. 36th Annu. Int. Conf. IEEE Eng. Med. Biol. Soc.*, 2014, pp. 4017–4021.

[27] W. Hong, "Transfemoral prosthesis control for inclined walking using impedance control and Bezier polynomial based optimization," Master's thesis, Elect. Comput. Eng., Texas A&M Univ., College Station, TX, USA, 2017.

[28] D. J. Villarreal and R. D. Gregg, "Unified phase variables of relative degree two for human locomotion," in *Proc. 38th Annu. Int. Conf. IEEE Eng. Med. Biol. Soc.*, 2016, pp. 6262–6267.

[29] H. Zhao, J. Reher, J. Horn, V. Paredes, and A. D. Ames, "Realization of nonlinear real-time optimization based controllers on self-contained transfemoral prosthesis," in *Proc. ACM/IEEE 6th Int. Conf. Cyber-Phys. Syst.*, 2015, pp. 130–138.

[30] S. Hood, M. K. Ishmael, A. Gunnell, K. Foreman, and T. Lenzi, "A kinematic and kinetic dataset of 18 above-knee amputees walking at various speeds," *Sci. Data*, vol. 7, no. 1, pp. 1–8, 2020.

[31] W. Hong, "A phase-shifting based human gait phase estimation for powered transfemoral prostheses [video]," Jan. 25, 2021. [Online]. Available: https://youtu.be/6JlfXk8XPRk

[32] A. Wolf, J. B. Swift, H. L. Swinney, and J. A. Vastano, "Determining lyapunov exponents from a time series," *Physica D Nonlinear Phenomena*, vol. 16, no. 3, pp. 285–317, 1985.

[33] A. H. Nayfeh and B. Balachandran, *Applied Nonlinear Dynamics: Analytical, Computational, and Experimental Methods*. Hoboken, NJ, USA: Wiley, 2008.

[34] J. B. Dingwell and J. P. Cusumano, "Nonlinear time series analysis of normal and pathological human walking," *Chaos Interdiscipl. J. Nonlinear Sci.*, vol. 10, no. 4, pp. 848–863, 2000.

[35] J. B. Dingwell, "Lyapunov exponents," in *Wiley encyclopedia of biomedical engineering*, Hoboken, New Jersey, USA: Wiley, 2006.

[36] H. Kantz and T. Schreiber, *Nonlinear time series analysis*. Cambridge, U.K.: Cambridge Univ. Press, 2004.

[37] R. Hegger, H. Kantz, and T. Schreiber, "Practical implementation of nonlinear time series methods: The TISEAN package," *Chaos Interdiscipl. J. Nonlinear Sci.*, vol. 9, no. 2, pp. 413–435, 1999.

[38] K. R. Embry, D. J. Villarreal, R. L. Macaluso, and R. D. Gregg, "Modeling the kinematics of human locomotion over continuously varying speeds and inclines," *IEEE Trans. Neural Syst. Rehabil. Eng.*, vol. 26, no. 12, pp. 2342–2350, Dec. 2018.